Long gamma-ray burst rate at very high redshift

Tomoya Kinugawa,[1], Yuichi Harikane,[2] and Katsuaki Asano[3]

[1] University of Tokyo
[2] National Astronomical Observatory of Japan
[3] Institute for cosmic ray research
E-mail: kinugawa@astro.s.u-tokyo.ac.jp

Abstract

Future missions for long gammma-ray burst (GRB) observations at high redshift such as HiZ-GUNDAM and THESEUS will provide clue to the star formation history in our universe. In this paper focusing on high redshift ($z > 8$) GRBs, we calculate the detection rate of long GRBs by future observations, considering both Population (Pop) I&II stars and Pop III stars as GRB progenitors. For the Pop I&II star formation rate (SFR), we adopt an up-to-date model of high-redshift SFR based on the halo mass function and dark matter accretion rate obtained from cosmological simulations. We show that the Pop I&II GRB rate steeply decreases with redshift. This would rather enable us to detect the different type of GRBs, Pop III GRBs, at very high redshift. If 10% or more Pop III stars die as an ultra-long GRB, the future missions would detect such GRBs in one year in spite of their low fluence. More luminous GRBs are expected from massive compact Pop III stars produced via the binary merger. In our conventional case, the detection rate of such luminous GRBs is 3-20 $\mathrm{yr}^{-1}(z > 8)$. Those future observations contribute to revealing of the Pop III star formation history.

Key words: High redshift, GRB rate, first star

1. Introduction

The long GRB at the highest redshift ever observed is GRB 090429B with a photometric redshift . There are future plans of long GRB observations at high redshift such as HiZ-GUNDAM (Yoshida et al. 2016) and THESEUS (Amati et al. 2018). Those observational missions can probe the high redshift universe. We have to identify what type of stars become long GRB progenitors to calculate the long GRB rate at high redshift. At present, the prediction of the GRB rate at $z > 10$ is difficult because of the lack of the observational knowledge of GRBs and the SFR at $z > 10$.

As the long GRB progenitor at high redshift, many authors have considered not only Population I and II (Pop I&II) stars, but also Population III (Pop III) stars. Pop III stars are first stars formed from the primordial gas with no metal. Since the mass distribution of Pop III stars is biased to heavier range than those for Pop I&II stars, we can expect that Pop III stars tend to launch long GRBs easily.

In this paper focusing on high redshift (> 8) GRBs, we calculate the detection rate of long GRBs by future observations, considering both Pop I&II stars and Pop III stars as GRB progenitors. The future detections of GRBs at very high redshift ($z > 10$) will unveil the star formation history in the very early era. For Pop I&II stars, we adopt an up-to-date model of high-redshift SFR proposed by Harikane et al. (2018) with the halo mass function and dark matter accretion rate obtained from cosmological simulations in Ishiyama et al. (2015).

On the other hand, in the case of Pop III stars, we consider both ultra-long GRBs from massive stars with heavy envelope and classical GRBs from massive compact stars, which experienced the binary merger.

2. Pop I/II GRB rate

In order to calculate the long GRB rate from Pop I&II stars at high redshift, first we estimate the cosmic star formation rate densities (SFRDs) of Pop I & II stars. Since the cosmic SFRDs at $z > 10$ is poorly constrained from observations, we consider two models in Behroozi & Silk (2015) and Harikane et al. (2018) for SFRDs.

Assuming that the GRB rate is proportional to the star formation rate, we extrapolate those rates from $z = 8$. The detection rate depends on the GRB spectrum, luminosity function, and energy band and sensitivity of instruments. The luminosity functions assumed in Wanderman & Piran (2010) and Lien et al. (2014); Lien et al. (2015). The GRB spectra are well described by the Band function, whose parameters are the peak energy ε_{pk}, low-energy index α, and high-energy index β. While the peak energy in the rest frame is assumed as a constant 511 keV in the analysis of Wanderman & Piran (2010), Lien et al. (2014); Lien et al. (2015) adopts a modified Yonetoku relation.

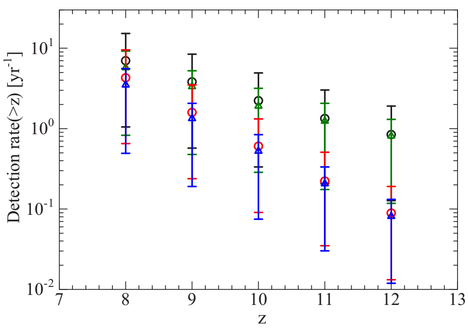

Fig. 1. The expectation of the GRB detection with an instrument with a sensitivity of 10^{-10} erg cm^{-2} s^{-1} in 0.5–4 keV, and field of view 0.2 str. Black and red circles are estimated with the parameters in Wanderman & Piran (2010) adopting the star formation rate in Behroozi & Silk (2015) and HPhi-1, respectively. Green and blue triangles are estimated with the parameters in Lien et al. (2015) adopting the star formation rate in Behroozi & Silk (2015) and HPhi-1, respectively.

As a future observation mission, we consider wide field X-ray monitor with Lobster Eye optics, which may be adopted by the missions in HiZ-GUNDAM or THESEUS. With such an instrument, we can expect a sensitivity of 10^{-10} erg cm^{-2} s^{-1} for 100 s exposure, and a field of view ~ 0.2 str [1] In Figure 1, we plot the expectation of the detection rate adopting the two models: the models in Wanderman & Piran (2010) (circles) and Lien et al. (2014); Lien et al. (2015) (triangles) for the GRB rate, luminosity function and spectral peak energy. If we adopt the star formation rate in Behroozi & Silk (2015) (black and green), both the models suggest a few GRB detection per year for $z > 10$. However, the Hphi-1 SFR, which seems consistent with the observed rate at $z \simeq 10$, leads to a detection rate $\ll 1$ for $z > 12$ (see red and blue symbols). In addition, we should take into account the efficiency of the redshift confirmation, which depends on the performance of the follow-up infrared telescope onboard HiZ-GUNDAM or THESEUS. The confirmation of GRBs at $z > 12$ seems not easy. However, in other words, this provides the opportunity to detect other types of trangient phenomena at high redshifts, such as GRBs from Pop III stars.

*1 Private communication with HiZ-GUNDAM working group. See also Yuan et al. (2016). Multiple Lobster Eye systems can enlarge the field of view depending on the budget in future plans. We conservatively assume single Lobster Eye system.

3. GRB from Pop III stars

3.1. Pop III star formation rate

At present, we have not significant constraint on the Pop III star formation rate from observations. However, the Pop III star formation rate has been estimated using the cosmological simulation. We consider two Pop III SFRDs in de Souza et al. 2011 and Inayoshi et al. 2016. The SFRD in de Souza et al. (2011) already conflicts with the limit by the Planck observation so that we adopt the SFRD in de Souza et al. (2011) decreasing by a factor of 0.3, which corresponds to the upper-limit of $\rho_{*,III}$ given by Inayoshi et al. (2016).

3.2. Ultra-long GRB rate from Pop III

Hereafter, we assume that the GRB rate is proportional to SFRDs. In the most optimistic scenario, all such heavy stars give rise to a GRB. Then, the apparent GRB rate is simply estimated as $f_B SFR/M_{\rm III}$, where f_B is the beaming factor. For metal free stars like Pop III stars, however, the stellar wind is suppressed so that a massive envelope remains at the collapse. In such cases, its long free fall time leads to ultra-long GRBs (Nakauchi et al. 2012, 2013), whose duration is $\sim 10^4$ s. Here, we adopt an optimistic opening angle $\theta_j = 20°$, which implies the beaming factor $f_B = 0.06$. Finally we obtain the comoving GRB rates at $z = 8$ as $\dot{n}_{GRB} = 1000$ Gpc^{-3} yr^{-1} and 440 Gpc^{-3} yr^{-1} for the SFRs in de Souza et al. (2011) and Inayoshi et al. (2016), respectively.

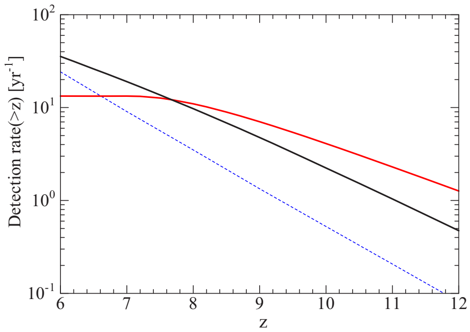

Fig. 2. The expectation of the ultra-long GRB detection originated from Pop III stars with an instrument with a sensitivity of 2×10^{-11} erg cm^{-2} s^{-1} in 0.5–4 keV, and FOV 0.2 str. The black and red lines are detection rates with SFRs of modified de Souza et al. (2011) and Inayoshi et al. (2016), respectively. The blue dashed line is the Pop I&II GRB rate with the HPhi-1 model.

The estimated detection rates of ultra-long GRBs are significantly higher than the usual GRB rate. The dominant sources in the HiZ-GUNDAM/THESEUS era may be ultra-long GRBs originated from Pop III stars. However, the assumption that all Pop III stars die as a GRB may be too optimistic. Practically the rates in Figure 4 are upper limits of Pop III ultra-long GRB rates. In this optimistic case, ultra-long GRBs from Pop III stars may be detected even at $z = 6 - 8$ especially for the modified de Souza SFRD model. If more than 10% of Pop III stars induce an ultra-long GRB, $\sim$ one detection per year is expected. de Souza et al. (2011) assumed that only 1% of Pop III stars cause a GRB at their end of life. Under such a conservative assumption, detection of an ultra-long GRB seems very difficult.

3.3. Classical GRB from Pop III merger

In order for classical long GRBs to occur, the progenitors need high angular momentum. Although the angular momentum of Pop III stars is unknown, the remnant of the binary merger during a common envelope (CE) phase possibly have a high angular momentum. When the radius of primary giant suddenly becomes larger or a radical mass transfer shrinks the orbit, the secondary star sometime plunges into the primary envelope. The secondary star spirals in and the envelope of primary will be evaporated. After the CE phase, the binary becomes a close binary or the two stars merges during a CE phase. In the latter case, the envelope evaporated, and a highly rotating helium star would remain (Fryer & Heger 2005). Furthermore, the highly spinning progenitors evolve as chemically homogeneous stars (Yoon et al. 2012). Since such highly rotating stars have small radius, the jet can break out the stellar surface with a high accretion rate like Pop I&II GRBs. For such idealized progenitors, GRBs can be as luminous as usual observed GRBs with duration of $\sim$ 10 s. Thus, we focus on the binary merger model (Fryer & Heger 2005) as the Pop III GRB progenitor. Figure 3 shows the expectation

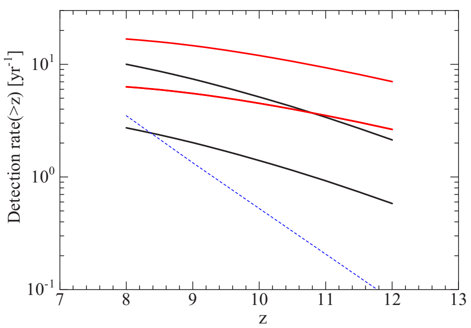

Fig. 3. The expectation of the classical GRB detection originated from Pop III stars based on the binary interaction model with an instrument with a sensitivity of 10^{-10} erg cm^2 s^{-1} in 0.5–4 keV, and a FOV 0.2 str. The black and red lines are detection rates with SFRs modified one in de Souza et al. (2011) and Inayoshi et al. (2016), respectively. The upper and lower lines correspond to the parameter of $\alpha\lambda = 0.1$ and 1, respectively. The blue dashed line is the Pop I&II GRB rate with the Hphi-1 model

of the classical GRB detection originated from Pop III stars based on the binary merger.

4. Conclusion & Discussion

In this paper, we consider the GRB from Pop III stars, using two SFRDs of Pop IIII considering the constraint from the Planck observation. We calculate the detection rate of Pop III GRBs by future observations such as HiZ-GUNDAM and THESEUS. In the pessimistic model, since the Pop III stars hold the hydrogen envelope because of the weak stellar wind, the Pop III stars are hard to launch a classical long GRB. In this case, Pop III stars might launch an ultra-long GRB. Only if more than 10% of Pop III stars launch a GRB jet, the future missions can detect such an ultra-long GRB per year.

However, many massive binary black holes confirmed by gravitational waves might be remnants of Pop III binaries (Kinugawa et al. 2014). If a significant fraction of Pop III stars are formed as a binary, we expect that highly rotating merged stars are formed via the binary merger, and they evolve as a chemically homogeneous star. Our population synthesis calculation shows that several % of Pop III binaries become such highly rotating stars which possibly launch a long GRB. If such highly rotating stars launch a classical GRB resembling low redshift long GRBs, they can be detected by HiZ-GUNDAM and THESEUS. Those future observations help us reveal the Pop III SFRD.

References

Amati, L., O'Brien, P., Götz, D., et al. 2018, Advances in Space Research, 62, 191

Behroozi, P. S., & Silk, J. 2015, ApJ, 799, 32

de Souza, R. S., Yoshida, N., & Ioka, K. 2011, A&A, 533, A32

Fryer, C. L., & Heger, A. 2005, ApJ, 623, 302

Harikane, Y., Ouchi, M., Ono, Y., et al. 2018, PASJ, 70, S11

Inayoshi, K., Kashiyama, K., Visbal, E., & Haiman, Z. 2016, MNRAS, 461, 2722

Ishiyama, T., Enoki, M., Kobayashi, M. A. R., et al. 2015, PASJ, 67, 61

Kinugawa, T., Inayoshi, K., Hotokezaka, K., Nakauchi, D., & Nakamura, T. 2014, MNRAS, 442, 2963

Lien, A., Sakamoto, T., Gehrels, N., et al. 2014, ApJ, 783, 24

Lien, A., Sakamoto, T., Gehrels, N., et al. 2015, ApJ, 806, 276

Nakauchi, D., Suwa, Y., Sakamoto, T., Kashiyama, K., & Nakamura, T. 2012, ApJ, 759, 128

Nakauchi, D., Kashiyama, K., Suwa, Y., & Nakamura, T. 2013, ApJ, 778, 67

Wanderman, D., & Piran, T. 2010, MNRAS, 406, 1944

Yoon, S.-C., Dierks, A., & Langer, N. 2012, A&A, 542, A113

Yoshida, K., Yonetoku, D., Sawano, T., et al. 2016, Proc. SPIE, 9905, 99050M